UCLA
UCLA Previously Published Works

Title

Segmental structural dynamics in Aβ42 globulomers.

Permalink

https://escholarship.org/uc/item/0mr3m43h

Authors

Yoon, Allison

Zhen, James

Guo, Zhefeng

Publication Date

2021-03-01

DOI

10.1016/j.bbrc.2021.01.081

Peer reviewed

# Segmental structural dynamics in Aβ42 globulomers

Allison Yoon, **James Zhen**, **Zhefeng Guo**[*]

Department of Neurology, Brain Research Institute, Molecular Biology Institute, University of California, Los Angeles, California 90095, USA.

Abstract

Aβ42 aggregation plays a central role in the pathogenesis of Alzheimer's disease. In addition to the insoluble fibrils that comprise the amyloid plaques, Aβ42 also forms soluble aggregates collectively called oligomers, which are more toxic and pathogenic than fibrils. Understanding the structure and dynamics of Aβ42 oligomers is critical for developing effective therapeutic interventions against these oligomers. Here we studied the structural dynamics of Aβ42 globulomers, a type of Aβ42 oligomers prepared in the presence of sodium dodecyl sulfate, using site-directed spin labeling. Spin labels were introduced, one at a time, at all 42 residue positions of Aβ42 sequence. Electron paramagnetic resonance spectra of spin-labeled samples reveal four structural segments based on site-dependent spin label mobility pattern. Segment-1 consists of residues 1-6, which have the highest mobility that is consistent with complete disorder. Segment-3 is the most immobilized region, including residues 31-34. Segment-2 and –4 have intermediate mobility and are composed of residues 7-30 and 35-42, respectively. Considering the inverse relationship between protein dynamics and stability, our results suggest that residues 31-34 are the most stable segment in Aβ42 oligomers. At the same time, the EPR spectral lineshape suggests that Aβ42 globulomers lack a well-packed structural core akin to that of globular proteins.

Graphical Abstract

Site-specific dynamics in Aβ42 globulomers
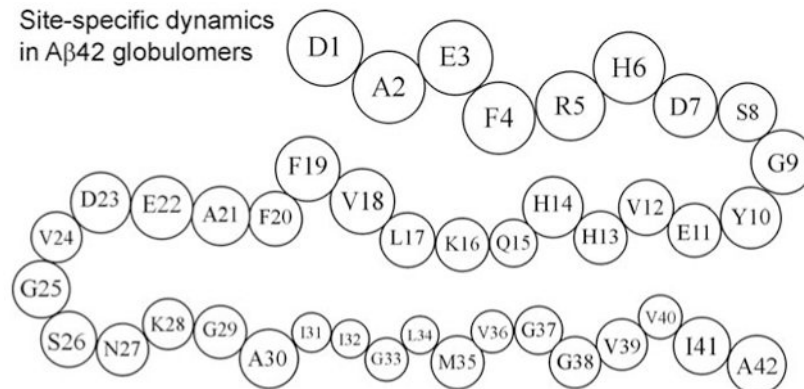
[*]To whom correspondence should be addressed: Zhefeng Guo, Department of Neurology, University of California, Los Angeles, 710 Westwood Plaza, Los Angeles, California 90095, USA. zhefeng@ucla.edu.

Keywords

Alzheimer's disease; Aβ42 oligomers; amyloid; neurodegenerative diseases; protein aggregation

INTRODUCTION

Aggregation of Aβ protein plays a central role in the pathogenesis of Alzheimer's disease [1,2]. The main products of Aβ aggregation include soluble oligomers and insoluble amyloid fibrils. The Aβ fibrils are the main component of senile plaques, but the oligomers are more toxic and believed to be more pathogenic than fibrils [3]. The mechanism of action by oligomers on neurons and neuronal processes is yet to be fully elucidated. To facilitate biochemical and biophysical studies of Aβ oligomers, different protocols have been devised to prepare in vitro oligomers with high homogeneity. Examples of these in vitro oligomers include Aβ-derived diffusible ligands [4], prefibrillar oligomers [5], amylospheroids [6], β-barrel pore-forming oligomers [7], and globulomers [8]. Globulomers, prepared in the presence of low concentrations of sodium dodecyl sulfate (SDS), have been shown to bind to hippocampal neurons and inhibit long-term potentiation [8]. Further studies showed that Aβ globulomers suppress spontaneous synaptic activity through inhibition of presynaptic calcium currents [9,10]. In tau transgenic mice, globulomers impair mitochondrial function [11]. Globulomer-specific antibodies showed positive staining in the brain slice of Alzheimer's disease patients, supporting the pathological relevance of Aβ globulomers [8,12].

Structural information of Aβ oligomers is important for understanding the process of oligomerization, the relationship between oligomers and fibrils, and eventually the structural basis of oligomer toxicity. Using site-directed spin labeling and electron paramagnetic resonance (EPR) spectroscopy, we previously studied the structure of Aβ42 globulomers with spin labels introduced, one at a time, at 14 residue positions [13]. X-ray powder diffraction and circular dichroism data showed primarily β-structures in Aβ42 globulomers. Intermolecular distance measurements using EPR suggested that residues 29-40 likely form an antiparallel β-sheet structure. Spin label mobility analysis revealed an overall increase in structural order from N- to C-terminus. Our findings are supported by solid-state NMR studies by Paravastu and colleagues [14], which show that residues 30-42 form a β-strand in an antiparallel β-sheet. Recently, new NMR data from Paravastu and colleagues [15] indicated that residues 11-24 forms another β-strand in an out-of-register parallel β-sheet. Despite these recent progresses, detailed structural models for globulomers are still beyond reach.

EPR is a commonly used structural technique for the studies of protein structure and dynamics [16,17]. The EPR spectral lineshape is primarily determined by spin label mobility, which reflects the local structure and dynamics at the labeling site. With decreasing spin label mobility, the overall amplitude of the EPR spectrum decreases and the separation between the two outermost peaks increases (Figure 1A). Using model proteins such as T4 lysozyme [18-20], the mobility of the spin label has been correlated to structural details revealed by the crystal structures of the spin-labeled proteins. Generally speaking, spin

labels located on protein surface have higher mobility than spin labels buried in the interior of proteins. Among the surface sites, spin labels located on a loop or turn structure are more mobile than spin labels located on α-helices or β-strands due to more rigid backbone structure. Figure 1 shows the correlation between EPR spectral lineshape and the local structure of the labeling site in three spin-labeled T4 lysozyme mutants, all of which have crystal structures available [18-20]. The EPR spectrum of T4 lysozyme A82R1 (R1 represents the spin label), a surface-facing turn site, gives rise to sharp spectral lines and high amplitude (Figure 1B). In comparison, the surface helix site S44R1 has an EPR spectrum that is broader with lower amplitude (Figure 1C). This is because the protein backbone of the α-helix is more rigid than that of a turn region. This increase in backbone order can be detected by EPR measurement. When the spin label is located in the interior of a protein, the EPR spectrum is characterized by increased separation between the two outmost peaks, which is labeled as $2A_{zz}$ in Figure 1D. A_{zz} is the Z-axis component of the hyperfine interaction between the unpaired electron and the nitrogen atom of the nitroxide spin label. For fast tumbling spin labels, only isotropic hyperfine interaction can be observed, shown in Figure 1A as A_0. The well-resolved A_{zz} is a feature of slow tumbling spin label, which is typically observed at buried sites where the spin label side chain is constrained by crowded local environment (Figure 1D).

To gain a detailed understanding into the segmental structural order and packing in Aβ42 globulomers, we completed a spin label scanning study to obtain EPR data on spin label mobility at the single-residue spatial resolution. Site-dependent spin label mobility shows that residues 1-6 are completely disordered and residues 31-34 are most rigid, suggesting that they form the most stable segment in Aβ42 globulomers. Meanwhile, the EPR spectral lineshape also suggests that globulomers do not have a well-packed structural core akin to that of globular proteins.

MATERIAL AND METHODS

Preparation of Aβ42 cysteine mutants and spin labeling.

Single cysteine mutants for all 42 residue positions of Aβ42 have been described previously [21,22]. For protein expression, the cysteine mutants of Aβ42 fusion protein construct, GroES-ubiquitin-Aβ42 [23], were transformed into *E. coli* C41 (DE3) cells (Lucigen). Detailed purification procedures have been described previously [25]. Briefly, expressed proteins were loaded on a nickel column in a high-pH denaturing buffer (50 mM phosphate, 8 M urea, pH 10) and eluted using an imidazole gradient. The fusion protein partners were then cleaved off with a deubiquitylating enzyme, Usp2-cc [24], resulting in the full-length Aβ42 protein without any extra residues. Following purification, the cysteine mutants of Aβ42 were labeled with the spin labeling reagent MTSSL, 1-oxyl-2,2,5,5-tetramethylpyrroline-3-methyl methanethiosulfonate (Adipogen), as previously described [13]. The spin label side chain is named R1. The labeling efficiency was evaluated with mass spectrometry. Only Aβ42 proteins with labeling efficiency of >95% were used in the subsequent experiments

Preparation of Aβ42 globulomers.

Aβ42 was dissolved in 100% 1,1,1,3,3,3-hexafluoro-2-propanol (HFIP) to 100 μM and incubated at room temperature for 24 h with shaking at 1000 rpm. Then HFIP was left to evaporate overnight in a fume hood. Aβ42 was then dissolved in dimethyl sulfoxide (DMSO) to a final concentration of 5 mM. Aβ concentration was determined using a fluorescamine method [26]. Then Aβ samples in DMSO were used to prepare globulomers as described previously [13].

EPR spectroscopy.

Approximately 15 μL of Aβ globulomer samples were loaded into glass capillaries (VitroCom) sealed at one end. Continuous-wave EPR spectra were collected using a Bruker EMXnano spectrometer at X-band at room temperature. A microwave power of 15 mW and a modulation frequency of 100 kHz were used. Modulation amplitude was optimized for each individual sample. Scan width was 100 G.

RESULTS AND DISCUSSION

We prepared 42 spin-labeled Aβ42 globulomer samples. Each sample consists of a variant of Aβ42 spin-labeled at a different residue position. Then we obtained the EPR spectra of all 42 globulomer samples, which are shown in Figure 2. All the EPR spectra are characterized by three sharp lines, characteristic of fast motion. These EPR spectra resembles the surface sites of T4 lysozyme (Figure 1), a model protein that has been extensively studied to correlate EPR spectral features and structural properties [18-20]. The hyperfine splitting in the EPR spectra of all the globulomers is also isotropic, as shown for the spectrum of A42R1 in Figure 2. The spin label motion has three main contributions: the tumbling of the Aβ oligomers, the protein backbone dynamics, and the internal bond rotations of the spin label side chain. Size exclusion chromatography studies showed that the main elution peak for Aβ42 globulomers was at approximately 150 kD [13]. Oligomers of >100 kD would have a rotational correlation time of >50 ns [27,28], which corresponds to very slow motion on the timescale of the continuous-wave EPR (Figure 1A). Therefore, the spin label mobility in the globulomers reflects mostly the motion of the protein backbone and the spin label side chain.

To obtain site-specific information on structural dynamics, we plotted the center line amplitude of the EPR spectra at each of the 42 labeling sites in Figure 3A. All the EPR spectra of spin-labeled globulomers have very similar lineshape with three sharp lines, suggesting fast motion. The difference in the spin label mobility can be captured in the overall amplitude of the EPR spectrum, which is represented by the center line amplitude (Figure 3A, inset). Based on their mobility, Aβ42 residues can be divided into four segments. The first six residues appear to be completely disordered, with highest spin label mobility. Residues 7-30 form a long segment of intermediate mobility, although this segment is more mobile than the C-terminal segment spanning residues 35-42. The residue positions with lowest spin label mobility are 31-34. Considering the inverse relationship between protein dynamics and stability [29,30], the EPR data suggest that residues 31-34 form the most stable segment in Aβ42 globulomers

In well-folded globular proteins, spin labels introduced at the hydrophobic core show characteristic slow-motion EPR spectra with well-separated outermost peaks ($2A_{zz}$), suggesting anisotropic hyperfine interactions (Figure 1D). In contrast, spin labels on the solvent-exposed surface sites show the two outermost peaks close together, indicating isotropic hyperfine interactions (A_0 in Figure 1A). In Aβ42 globulomers, even the most rigid labeling positions, 31-34, give rise to EPR spectra with isotropic hyperfine interactions (Figure 2), suggesting relatively unrestrained motion for the spin label side chains. Therefore, the EPR spectral features suggest that Aβ42 globulomers lack a well-packed structural core akin to that of globular proteins.

In a previous study of our group [13], we introduced spin labels at 14 residue positions of Aβ42 and studied the spin label mobility in globulomers. In that study [13], globulomers were prepared using a mixture of spin-labeled and wild-type Aβ42 proteins, a procedure called spin dilution. As a result, the intermolecular spin-spin interactions were minimized, allowing the determination of rotational correlation time using spectral simulations. In the present study, the globulomers were prepared using only spin-labeled Aβ42 proteins, so the intermolecular spin-spin interactions also contribute to the EPR spectral lineshape. To investigate if the EPR spectra of globulomers formed by only spin-labeled Aβ42 give similar information on spin label mobility as the EPR spectra of Aβ42 globulomers with spin dilution, we reproduced the graph of rotational correlation time from the previous study of Gu et al. [13] (Figure 3B). Comparison of Figure 3A and 3B indicates that the EPR center line amplitude from only spin-labeled Aβ42 (Figure 3A) captures the spin label mobility information shown in Figure 3B. This comparison also reveals the power of increased spatial resolution. The previous study [13] revealed the general trend of increasing structural order from N- to C-terminus, but the present study reveals detailed structural segments with distinct spin label mobility patterns.

Using spin labeling and EPR, our group previously studied another type of Aβ42 oligomer preparation in Gu et al. [31]. Although the oligomers were prepared using a fusion protein construct of Aβ42, the oligomers had properties of prefibrillar oligomers such as binding to oligomer-specific A11 antibody [31]. The spin label mobility data for the prefibrillar oligomers, reproduced in Figure 3C, are markedly different from globulomers. The prefibrillar Aβ42 oligomers [31] show two segments of low mobility residues (13-23 and 28-42), which are separated by a high-mobility segment (Figure 3C). This is consistent with a β-turn-β motif. The same β-turn-β motif has also been suggested in Aβ42 fibrils from hydrogen exchange data [32,33], suggesting a potential structural conversion from oligomers to fibrils through "strand rotation" [31]. Another difference between globulomers and the previously studied prefibrillar oligomers [31] is that the EPR spectra of prefibrillar oligomers are as immobilized as those in the buried sites of globular proteins, suggesting well-packed structures in the prefibrillar oligomers. An example of these immobilized spectra is shown in Figure 3C (inset).

Paravastu and colleagues have studied an oligomer preparation of Aβ42, called 150-kD oligomers, using solid-state NMR techniques [14,15]. Similar to Aβ42 globulomers [8], the 150-kD oligomers were also prepared in the presence of low concentrations of SDS and showed 30-60 kD bands on SDS-PAGE [34,35]. In our previous studies, we found that Aβ42

globulomers had a main peak at approximately 150 kD on size exclusion chromatography chromatogram [13]. These studies suggest that globulomers and the 150-kD oligomers are the same type of Aβ42 oligomers. Results obtained by Paravastu and colleagues showed the 150-kD oligomers have two β-strands at residues 11-24 and 30-42 [14,15]. This is consistent with our previous findings on prefibrillar oligomers (Figure 3C) [31], which showed two low mobility regions at residues 13-23 and 28-42. In a recent solid-state NMR study of β-barrel pore-forming Aβ42 oligomers, Carulla and colleagues revealed two different Aβ42 subunits in the oligomers: one subunit consisting of two β-strands at residues 9-21 and 28-40 and the other one with only one β-strand at residues 29-31 [36]. Collectively, these studies suggest two potential β-strand regions at residues 10-20 and 30-42. The continuous β-strand at residues 30-42 is particularly in contrast to the β-turn-β motif of this region in Aβ42 fibril structures [37-41]. Therefore, in addition to antiparallel β-sheet structure, the continuous C-terminal β-strand at residues 30-40 may be another signature structural feature for Aβ42 oligomers in general.

Our EPR data also suggest that the two hydrophobic regions of Aβ42 sequence, residues 17-21 (also known as the central hydrophobic cluster) and 30-42, play different roles in the oligomers. The overall mobility of the C-terminal hydrophobic region covering residues 30-42 is lower than the central hydrophobic cluster residues 17-21 (Figure 3A). This suggests that the C-terminal hydrophobic region contributes more to the stability of Aβ42 globulomers. The four residues with lowest spin label mobility include two isoleucine, one leucine, and one glycine residues, suggesting that Aβ42 globulomers are stabilized primarily by hydrophobic interactions. In a previous cysteine scanning mutagenesis study of Aβ42 oligomerization in the presence of 8 M urea, we found that mutations to C-terminal residues Ile-31, Ile-32, Leu-34, Val-39, Val-40 and Ile-41 abolished the formation of SDS-resistant tetramer and hexamers, but mutations to residues Leu-17 and Phe-20 did not have the same effect [42]. This is also consistent with a previous hydrogen exchange study of Aβ42 globulomers, which showed that the C-terminal residues 31-41 are the only long stretch of protected residues [43]. Collectively, these results suggest that, although residues 7-30 are ordered in Aβ42 globulomers, C-terminal residues 31-42 contribute most to the structural stability, with residues 31-34 at the structural core.

ACKNOWLEDGEMENTS

REFERENCES

[1]. Scheltens P, Blennow K, Breteler MMB, de Strooper B, Frisoni GB, Salloway S, Van der Flier WM, Alzheimer's disease, Lancet. 388 (2016) 505–517. 10.1016/S0140-6736(15)01124-1. [PubMed: 26921134]

[2]. Sinnige T, Stroobants K, Dobson CM, Vendruscolo M, Biophysical studies of protein misfolding and aggregation in in vivo models of Alzheimer's and Parkinson's diseases, Q. Rev. Biophys 53 (2020) e10 10.1017/S0033583520000025.

[3]. Benilova I, Karran E, Strooper BD, The toxic Aβ oligomer and Alzheimer's disease: an emperor in need of clothes, Nat. Neurosci 15 (2012) 349–357. 10.1038/nn.3028. [PubMed: 22286176]

[4]. Lambert MP, Barlow AK, Chromy BA, Edwards C, Freed R, Liosatos M, Morgan TE, Rozovsky I, Trommer B, Viola KL, Wals P, Zhang C, Finch CE, Krafft GA, Klein WL, Diffusible, nonfibrillar ligands derived from Aβ1–42 are potent central nervous system neurotoxins, Proc Natl Acad Sci U S A. 95 (1998) 6448–6453. [PubMed: 9600986]

[5]. Kayed R, Head E, Thompson JL, McIntire TM, Milton SC, Cotman CW, Glabe CG, Common structure of soluble amyloid oligomers implies common mechanism of pathogenesis, Science. 300 (2003) 486–489. 10.1126/science.1079469. [PubMed: 12702875]

[6]. Hoshi M, Sato M, Matsumoto S, Noguchi A, Yasutake K, Yoshida N, Sato K, Spherical aggregates of beta-amyloid (amylospheroid) show high neurotoxicity and activate tau protein kinase I/ glycogen synthase kinase-3beta, Proc. Natl. Acad. Sci. U.S.A 100 (2003) 6370–6375. 10.1073/ pnas.1237107100. [PubMed: 12750461]

[7]. Serra-Batiste M, Ninot-Pedrosa M, Bayoumi M, Gairí M, Maglia G, Carulla N, Aβ42 assembles into specific β-barrel pore-forming oligomers in membrane-mimicking environments, Proc. Natl. Acad. Sci. U.S.A (2016). 10.1073/pnas.1605104113.

[8]. Barghorn S, Nimmrich V, Striebinger A, Krantz C, Keller P, Janson B, Bahr M, Schmidt M, Bitner RS, Harlan J, Barlow E, Ebert U, Hillen H, Globular amyloid β-peptide1–42 oligomer – a homogenous and stable neuropathological protein in Alzheimer's disease, J. Neurochem 95 (2005) 834–847. 10.1111/j.1471-4159.2005.03407.x. [PubMed: 16135089]

[9]. Nimmrich V, Grimm C, Draguhn A, Barghorn S, Lehmann A, Schoemaker H, Hillen H, Gross G, Ebert U, Bruehl C, Amyloid β oligomers (Aβ(1-42) globulomer) suppress spontaneous synaptic activity by inhibition of P/Q-type calcium currents, J. Neurosci 28 (2008) 788–797. 10.1523/ JNEUROSCI.4771-07.2008. [PubMed: 18216187]

[10]. Hermann D, Mezler M, Müller MK, Wicke K, Gross G, Draguhn A, Bruehl C, Nimmrich V, Synthetic Aβ oligomers (Aβ1–42 globulomer) modulate presynaptic calcium currents: Prevention of Aβ-induced synaptic deficits by calcium channel blockers, European Journal of Pharmacology. 702 (2013) 44–55. 10.1016/j.ejphar.2013.01.030. [PubMed: 23376566]

[11]. Eckert A, Hauptmann S, Scherping I, Meinhardt J, Rhein V, Dröse S, Brandt U, Fändrich M, Müller W, Götz J, Oligomeric and fibrillar species of β-amyloid (Aβ42) both impair mitochondrial function in P301L tau transgenic mice, J Mol Med. 86 (2008) 1255–1267. 10.1007/s00109-008-0391-6. [PubMed: 18709343]

[12]. Hillen H, Barghorn S, Striebinger A, Labkovsky B, Müller R, Nimmrich V, Nolte MW, Perez-Cruz C, van der Auwera I, van Leuven F, van Gaalen M, Bespalov AY, Schoemaker H, Sullivan JP, Ebert U, Generation and Therapeutic Efficacy of Highly Oligomer-Specific β-Amyloid Antibodies, J. Neurosci 30 (2010) 10369–10379. 10.1523/JNEUROSCI.5721-09.2010. [PubMed: 20685980]

[13]. Gu L, Liu C, Guo Z, Structural insights into Aβ42 oligomers using site-directed spin labeling, J. Biol. Chem 288 (2013) 18673–18683. 10.1074/jbc.M113.457739. [PubMed: 23687299]

[14]. Huang D, Zimmerman MI, Martin PK, Nix AJ, Rosenberry TL, Paravastu AK, Antiparallel β-sheet structure within the C-terminal region of 42-residue Alzheimer's β-amyloid peptides when they form 150 kDa oligomers, J. Mol. Biol 427 (2015) 2319–2328. 10.1016/j.jmb.2015.04.004. [PubMed: 25889972]

[15]. Gao Y, Guo C, Watzlawik JO, Randolph PS, Lee EJ, Huang D, Stagg SM, Zhou H-X, Rosenberry TL, Paravastu AK, Out-of-register parallel β-sheets and antiparallel β-sheets coexist in 150 kDa oligomers formed by Amyloid-β(1-42), J. Mol. Biol (2020). 10.1016/j.jmb.2020.05.018.

[16]. Hubbell WL, López CJ, Altenbach C, Yang Z, Technological advances in site-directed spin labeling of proteins, Curr. Opin. Struct. Biol 23 (2013) 725–733. 10.1016/j.sbi.2013.06.008. [PubMed: 23850140]

[17]. Cafiso DS, Identifying and quantitating conformational exchange in membrane proteins using site-directed spin labeling, Acc. Chem. Res 47 (2014) 3102–3109. 10.1021/ar500228s. [PubMed: 25152957]

[18]. Fleissner MR, Cascio D, Hubbell WL, Structural origin of weakly ordered nitroxide motion in spin-labeled proteins, Protein Sci. 18 (2009) 893–908. 10.1002/pro.96. [PubMed: 19384990]

[19]. Guo Z, Cascio D, Hideg K, Hubbell WL, Structural determinants of nitroxide motion in spin-labeled proteins: Solvent-exposed sites in helix B of T4 lysozyme, Protein Sci. 17 (2008) 228–239. 10.1110/ps.073174008. [PubMed: 18096642]

[20]. Guo Z, Cascio D, Hideg K, Kálái T, Hubbell WL, Structural determinants of nitroxide motion in spin-labeled proteins: Tertiary contact and solvent-inaccessible sites in helix G of T4 lysozyme, Protein Sci. 16 (2007) 1069–1086. 10.1110/ps.062739107. [PubMed: 17473014]

[21]. Wang H, Lee YK, Xue C, Guo Z, Site-specific structural order in Alzheimer's Aβ42 fibrils, R. Soc. Open Sci 5 (2018) 180166 10.1098/rsos.180166. [PubMed: 30109072]

[22]. Wang H, Duo L, Hsu F, Xue C, Lee YK, Guo Z, Polymorphic Aβ42 fibrils adopt similar secondary structure but differ in cross-strand side chain stacking interactions within the same β-sheet, Sci Rep. 10 (2020) 5720 10.1038/s41598-020-62181-x. [PubMed: 32235842]

[23]. Shahnawaz M, Thapa A, Park I-S, Stable activity of a deubiquitylating enzyme (Usp2-cc) in the presence of high concentrations of urea and its application to purify aggregation-prone peptides, Biochem. Biophys. Res. Commun 359 (2007) 801–805.10.1016/j.bbrc.2007.05.186. [PubMed: 17560941]

[24]. Baker RT, Catanzariti A-M, Karunasekara Y, Soboleva TA, Sharwood R, Whitney S, Board PG, Using deubiquitylating enzymes as research tools, Meth. Enzymol 398 (2005) 540–554. 10.1016/S0076-6879(05)98044-0.

[25]. Agopian A, Guo Z, Structural origin of polymorphism of Alzheimer's amyloid β-fibrils, Biochem. J 447 (2012) 43–50. 10.1042/BJ20120034. [PubMed: 22823461]

[26]. Xue C, Lee YK, Tran J, Chang D, Guo Z, A mix-and-click method to measure amyloid-β concentration with sub-micromolar sensitivity, R. Soc. Open Sci 4 (2017) 170325 10.1098/rsos.170325. [PubMed: 28878984]

[27]. Ryabov YE, Geraghty C, Varshney A, Fushman D, An efficient computational method for predicting rotational diffusion tensors of globular proteins using an ellipsoid representation, J Am Chem Soc. 128 (2006) 15432–15444. 10.1021/ja062715t. [PubMed: 17132010]

[28]. Su X-C, Jergic S, Ozawa K, Burns ND, Dixon NE, Otting G, Measurement of dissociation constants of high-molecular weight protein-protein complexes by transferred 15N-relaxation, J Biomol NMR. 38 (2007) 65–72. 10.1007/s10858-007-9147-9. [PubMed: 17390106]

[29]. Tsai AM, Udovic TJ, Neumann DA, The inverse relationship between protein dynamics and thermal stability., Biophys J. 81 (2001) 2339–2343. [PubMed: 11566803]

[30]. Chung JK, Thielges MC, Fayer MD, Conformational dynamics and stability of HP35 studied with 2D IR vibrational echoes, J Am Chem Soc. 134 (2012) 12118–12124. 10.1021/ja303017d. [PubMed: 22764745]

[31]. Gu L, Liu C, Stroud JC, Ngo S, Jiang L, Guo Z, Antiparallel triple-strand architecture for prefibrillar Aβ42 oligomers, J. Biol. Chem 289 (2014) 27300–27313. 10.1074/jbc.M114.569004. [PubMed: 25118290]

[32]. Lührs T, Ritter C, Adrian M, Riek-Loher D, Bohrmann B, Döbeli H, Schubert D, Riek R, 3D structure of Alzheimer's amyloid-β(1-42) fibrils, Proc. Natl. Acad. Sci. U.S.A 102 (2005) 17342–17347. 10.1073/pnas.0506723102. [PubMed: 16293696]

[33]. Olofsson A, Sauer-Eriksson AE, Öhman A, The solvent protection of Alzheimer amyloid-β-(1–42) fibrils as determined by solution NMR spectroscopy, J. Biol. Chem 281 (2006) 477–483. 10.1074/jbc.M508962200. [PubMed: 16215229]

[34]. Rangachari V, Moore BD, Reed DK, Sonoda LK, Bridges AW, Conboy E, Hartigan D, Rosenberry TL, Amyloid-β(1–42) Rapidly Forms Protofibrils and Oligomers by Distinct Pathways in Low Concentrations of Sodium Dodecylsulfate†, Biochemistry. 46 (2007) 12451–12462. 10.1021/bi701213s. [PubMed: 17910477]

[35]. Moore BD, Rangachari V, Tay WM, Milkovic NM, Rosenberry TL, Biophysical Analyses of Synthetic Amyloid-β(1–42) Aggregates before and after Covalent Cross-Linking. Implications for Deducing the Structure of Endogenous Amyloid-β Oligomers, Biochemistry. 48 (2009) 11796–11806. 10.1021/bi901571t. [PubMed: 19916493]

[36]. Ciudad S, Puig E, Botzanowski T, Meigooni M, Arango AS, Do J, Mayzel M, Bayoumi M, Chaignepain S, Maglia G, Cianferani S, Orekhov V, Tajkhorshid E, Bardiaux B, Carulla N, Aβ(1-42) tetramer and octamer structures reveal edge conductivity pores as a mechanism for membrane damage, Nat Commun. 11 (2020) 3014 10.1038/s41467-020-16566-1. [PubMed: 32541820]

[37]. Gu L, Tran J, Jiang L, Guo Z, A new structural model of Alzheimer's Aβ42 fibrils based on electron paramagnetic resonance data and Rosetta modeling, J. Struct. Biol 194 (2016) 61–67. 10.1016/j.jsb.2016.01.013. [PubMed: 26827680]

[38]. Xiao Y, Ma B, McElheny D, Parthasarathy S, Long F, Hoshi M, Nussinov R, Ishii Y, Aβ(1-42) fibril structure illuminates self-recognition and replication of amyloid in Alzheimer's disease, Nat. Struct. Mol. Biol 22 (2015) 499–505. 10.1038/nsmb.2991. [PubMed: 25938662]

[39]. Colvin MT, Silvers R, Ni QZ, Can TV, Sergeyev IV, Rosay M, Donovan KJ, Michael B, Wall JS, Linse S, Griffin RG, Atomic resolution structure of monomorphic Aβ42 amyloid fibrils, J. Am. Chem. Soc 138 (2016) 9663–9674. 10.1021/jacs.6b05129. [PubMed: 27355699]

[40]. Wälti MA, Ravotti F, Arai H, Glabe CG, Wall JS, Böckmann A, Güntert P, Meier BH, Riek R, Atomic-resolution structure of a disease-relevant Aβ(1-42) amyloid fibril, Proc. Natl. Acad. Sci. U.S.A 113 (2016) E4976–E4984. 10.1073/pnas.1600749113. [PubMed: 27469165]

[41]. Gremer L, Schölzel D, Schenk C, Reinartz E, Labahn J, Ravelli RBG, Tusche M, Lopez-Iglesias C, Hoyer W, Heise H, Willbold D, Schröder GF, Fibril structure of amyloid-ß(1-42) by cryo-electron microscopy, Science. 358 (2017) 116–119. 10.1126/science.aao2825. [PubMed: 28882996]

[42]. Ngo S, Guo Z, Key residues for the oligomerization of Aβ42 protein in Alzheimer's disease, Biochem. Biophys. Res. Commun 414 (2011) 512–516. 10.1016/j.bbrc.2011.09.097. [PubMed: 21986527]

[43]. Yu L, Edalji R, Harlan JE, Holzman TF, Lopez AP, Labkovsky B, Hillen H, Barghorn S, Ebert U, Richardson PL, Miesbauer L, Solomon L, Bartley D, Walter K, Johnson RW, Hajduk PJ, Olejniczak ET, Structural characterization of a soluble amyloid β-peptide oligomer, Biochemistry. 48 (2009) 1870–1877. 10.1021/bi802046n. [PubMed: 19216516]

- Aβ42 globulomers are a type of toxic and physiologically relevant oligomers.

- We used spin labeling and EPR to obtain mobility information at all 42 sites.

- Residues 1-6 are disordered; 7-30 and 35-42 are two of the ordered segments.

- Residues 31-34 comprise the most stable segment in globulomers.

- Globulomers don't have a well-packed structural core like globular proteins.
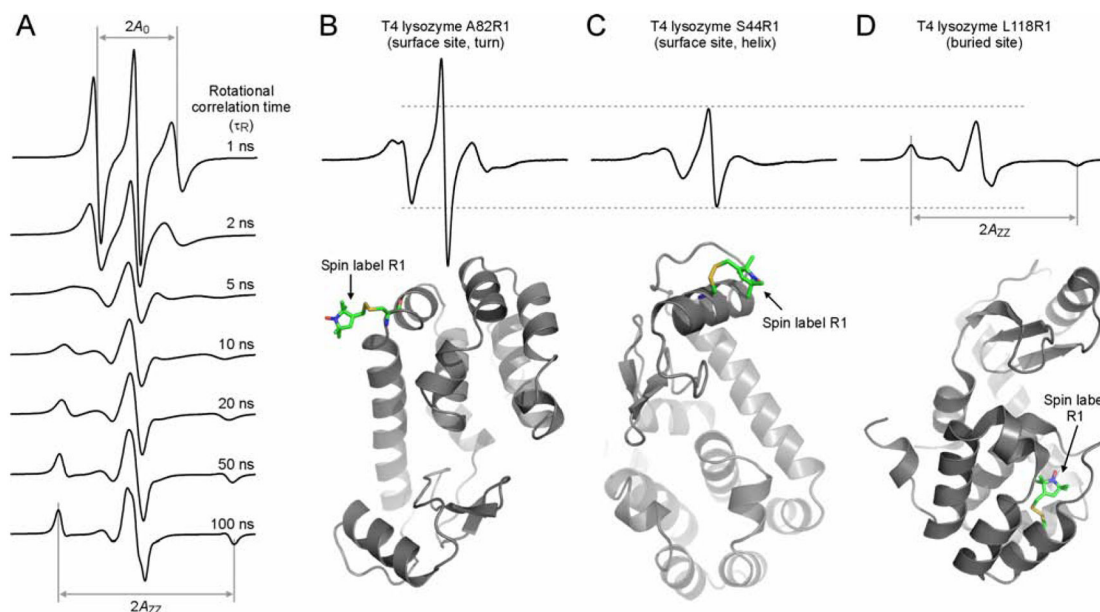
Figure 1. Effect of spin label mobility and labeling location on EPR spectral lineshape.
(*A*) Effect of spin label mobility on the EPR spectral lineshape. EPR spectra were simulated using isotropic spin label motion with rotational correlation time (τ_R) of 1 to 100 ns. Note that increase in rotational correlation time from 1 to 5 ns leads to reduced spectral amplitude. Further increase in rotational correlation time above 5 ns results in increased separation between the two outermost peaks. At fast motions (τ_R of 1-5 ns), only the isotropic hyperfine splitting, A_0, can be measured from the EPR spectrum. At slower motions (τ_R >10 ns), the z-axis component of the hyperfine splitting, A_{zz}, can be measured from the EPR spectrum. (*B-D*) Effect of the labeling location on EPR spectral lineshape. R1 represents the spin label. Dashed lines are drawn to aid comparison. The ribbon models are built from the crystal structures of the T4 lysozyme variants, A82R1 (PDB entry 1ZYT) [18], S44R1 (PDB entry 2Q9E) [19], and L118R1 (2NTH) [20]. All EPR spectra are 100 G in width.
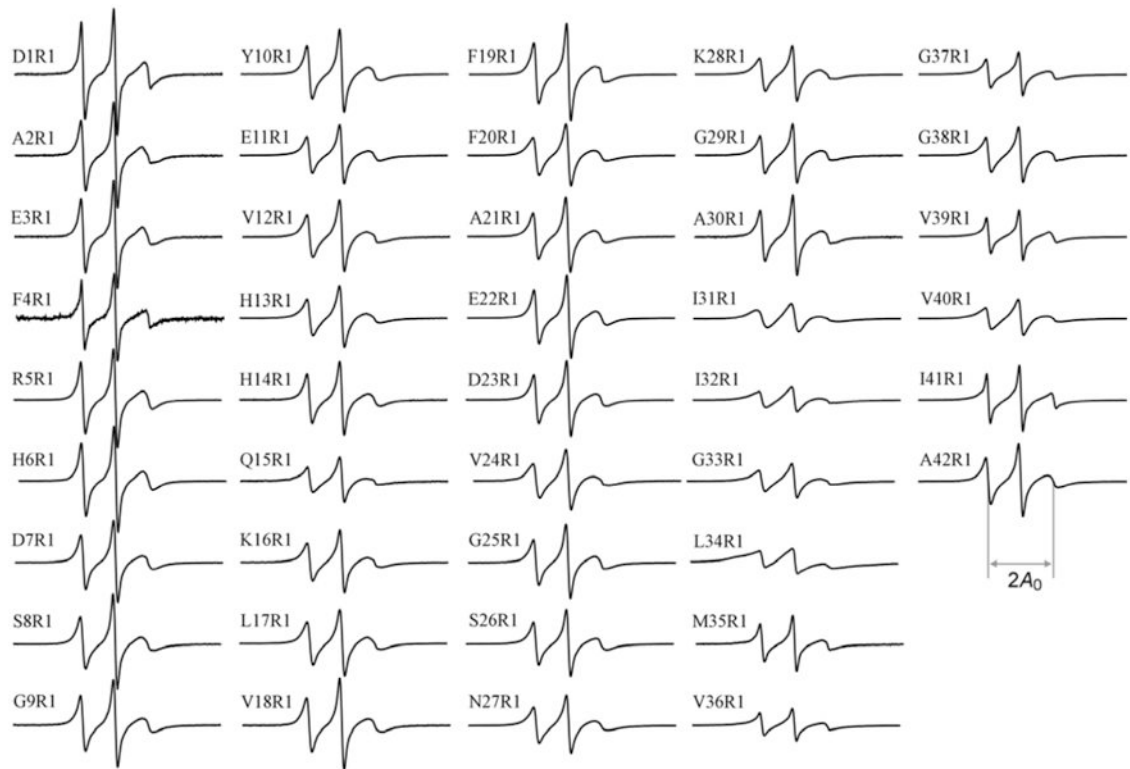
Figure 2. EPR spectra of spin-labeled Aβ42 globulomers.
R1 represents the spin label. Measurement of the isotropic hyperfine splitting, A_0, is shown for the EPR spectrum of A42R1. All spectra are normalized to the same number of spins. The scan width is 100 G
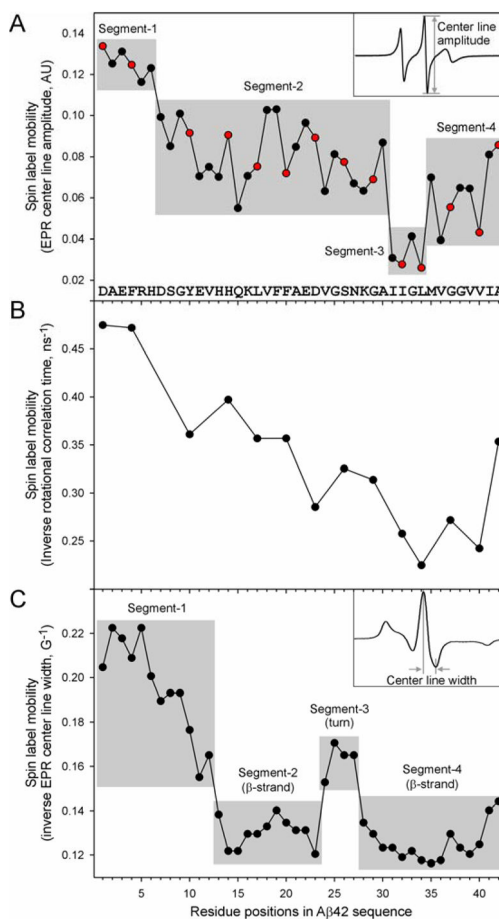
Figure 3. Segmental structural dynamics in Aβ42 globulomers.
(*A*) Residue-dependent profile of the EPR center line amplitude in spin-labeled Aβ42 globulomers. Higher EPR spectral amplitude corresponds to higher spin label mobility, suggesting that the labeling site is more disordered. In contrast, lower EPR spectral amplitude suggests lower spin label mobility and more structural order at the labeling site. Based on this analysis, the Aβ42 sequence can be grouped into four segments. Segment-1 includes residues 1-6 and is likely completely disordered. Segment-3 consists of residues 31-34 and is the most ordered region in Aβ42 globulomers. Inset shows the measurement of center line amplitude. Symbols in red represent residue positions also studied in a previous work [13] (see also panel *B*). AU, arbitrary unit. (*B*) Spin label mobility analysis in a previous EPR study of Aβ42 globulomers [13] that includes 14 labeling positions. Note that the results of this work (panel *A*) are inline with our previous study, suggesting high reproducibility of our EPR data. (*C*) Spin label mobility analysis in a previous EPR study of Aβ42 prefibrillar oligomers [31], showing two clear segments of low spin label mobility (segments 2 and 4) that are separated by a high mobility segment.